http://dx.doi.org/10.5012/bkcs.2014.35.4.1195

Role of HCl in Atomic Layer Deposition of TiO_2 Thin Films from Titanium Tetrachloride and Water

Jina Leem,[a] Inhye Park,[a] Yinshi Li, Wenhao Zhou, Zhenyu Jin, Seokhee Shin, and Yo-Sep Min[*]

Department of Chemical Engineering, Konkuk University, Seoul 143-701, Korea. [*]E-mail: ysmin@konkuk.ac.kr
Received January 28 2014, Accepted February 5, 2014

Atomic layer deposition (ALD) of TiO_2 thin film from $TiCl_4$ and H_2O has been intensively studied since the invention of ALD method to grow thin films *via* chemical adsorptions of two precursors. However the role of HCl which is a gaseous byproduct in ALD chemistry for TiO_2 growth is still intriguing in terms of the growth mechanism. In order to investigate the role of HCl in TiO_2 ALD, HCl pulse and its purging steps are inserted in a typical sequence of $TiCl_4$ pulse-purge-H_2O pulse-purge. When they are inserted after the first-half reaction (chemisorption of $TiCl_4$), the grown thickness of TiO_2 becomes thinner or thicker at lower or higher growth temperatures than 300 °C, respectively. However the insertion after the second-half reaction (chemisorption of H_2O) results in severely reduced thicknesses in all growth temperatures. By using the result, we explain the growth mechanism and the role of HCl in TiO_2 ALD.

Key Words : TiO_2, Atomic layer deposition, HCl, $TiCl_4$, H_2O

Introduction

Atomic layer deposition (ALD) is a special modification of chemical vapor deposition (CVD) to grow various thin films *via self-limiting chemisorption*.[1-3] While in CVD an appropriate precursor vapor and a reaction gas are simultaneously supplied to a substrate, in ALD they are alternately exposed onto the substrate of which temperature is maintained to be low enough in order to avoid thermal decomposition of the precursor. The ALD reactor is purged with an inert gas between the exposures of the precursor vapor and the reaction gas. Each cycle of ALD process generally consists of precursor exposure - purge - reaction gas exposure - purge. Therefore, the film grows through chemisorption between the gaseous molecules (*i.e.*, precursor vapor or reactant gas) and reactive functional groups on the surface (*i.e.*, hydroxyl groups or chemisorbed organometallic groups). Once vacant adsorption sites are saturated by adsorbate molecules to form one monolayer (practically sub-monolayer is formed due to the bulkiness of adsorbate molecules), the precursor or reactant in excess do not chemically adsorb on the monolayer. Consequently the film grows *via* the self-limiting mechanism.

For an ideal ALD process, several characteristics are required in ALD chemistry: (1) the chemisorption should be highly exothermic with a high activation of desorption (E_d) in order to guarantee 100% sticking coefficient in the chemisorption, (2) byproducts should not chemically re-adsorb on the vacant sites after the chemisorption, and (3) the byproduct should not etch the growing film through a series of reverse reactions of the growth. In terms of these requirements, the chemistry for ALD of Al_2O_3 from trimethylaluminum (TMA) and water is nearly ideal. It shows extremely high reaction enthalpies of chemisorption with high E_d values for both the first- and second-half reactions. For the first half-reaction between Al–OH and TMA, the enthalpy change is around −1.70 eV (E_d = 1.61 eV), and for the second-half reaction between Al–$(CH_3)_2$ and H_2O, it is around −1.48 eV (E_d = 1.61 eV).[4] Furthermore methane (the byproduct in the first- and second-half reactions) does not chemically re-adsorb on the surface and is not able to etch the growing film. However many precursors for ALD rather show deviation from the ideal ALD chemistry.

TiO_2 ALD from titanium tetrachloride ($TiCl_4$) and water is an example for the non-ideal ALD. Several groups had theoretically or experimentally studied the chemistry of TiO_2 ALD.[5-13] In the generally accepted mechanism of TiO_2 growth, $TiCl_4$ mainly reacts with the surface OH groups releasing HCl in the first-half reaction:

$$\text{n(-OH)(s)} + \text{TiCl}_4\text{(g)} \rightarrow \text{(-O-)}_n\text{TiCl}_{4-n}\text{(s)} + \text{nHCl(g)} \quad (1)$$

where (s) denotes surface. The adsorbed chlorotitanium ($TiCl_x$) species may react with water releasing HCl again in the second-half reaction, which results in the recovery of the surface OH groups for the next cycle:

$$\text{(-O-)}_n\text{TiCl}_{4-n}\text{(s)} + \text{(4-n)H}_2\text{O(g)} \rightarrow \text{(-O-)}_n\text{Ti(OH)}_{4-n}\text{(s)} + \text{(4-n)HCl(g)} \quad (2)$$

Because the growth of TiO_2 is mainly contributed from the surface exchange reactions (Eqs. 1 and 2), the surface OH groups play a key role in the ALD sequence. There are two kinds of OH groups on the surface of oxides: isolated OH and adjacent hydrogen-bonded OH (H-boned OH) groups. The H-bonded OH groups are dominant at low temperatures, but they are condensed at high temperatures by dehydroxylation to form oxygen bridges liberating H_2O:

[a]These authors contributed equally to this work.

$$\text{Ti(-OH)-O-Ti(OH)(s)} \rightarrow \text{Ti(-O-)}_2\text{Ti(s)} + \text{H}_2\text{O(g)} \quad (3)$$

The oxygen bridges, formed by Eq. (3), may also contribute to the first-half reaction of TiO_2 ALD at high temperatures though the dissociative chemisorption of $TiCl_4$:

$$\text{Ti(-O-)}_2\text{Ti(s)} + \text{TiCl}_4\text{(g)} \rightarrow \text{Ti(Cl)-O-Ti(OTiCl}_3\text{)(s)} \quad (4)$$

In Eqs. (1) and (2), when n = 1 and n = 2, the reactions are monofunctional and bifunctional, respectively. The monofunctional and bifunctional reactions produce gaseous HCl as a byproduct. However HCl is not released in the dissociative chemisorption (Eq. 4).

Although ALD of TiO_2 from $TiCl_4$ and water has been intensively investigated since the invention of the ALD method,[14-27] the role of HCl is not clear yet. Here we investigate the role of HCl which may be one of origins for the non-ideality in TiO_2 ALD.

Experimental

All thin films were grown on boron doped *p*-type (100) Si wafers, of which resistivity is 5-20 Ω-cm, by using a laminar flow type ALD reactor (ATOMIC-CLASSIC 2nd edition, CN-1 Co., Ltd.). Although our reactor could process a 6 in. wafer, five square specimens (2 × 2 cm^2) were loaded on the center, left, right, top and bottom positions of the 6 in. substrate holder in order to evaluate non-uniformity in the 6 in. wafer. The specimens were used without removing the native oxide. $TiCl_4$ (UP Chemical Co., Ltd) and water were vaporized from external canisters at room temperature and led into the reactor through solenoid valves without any carrier gas. The doses of $TiCl_4$ and water were ~2.9×10^{-6} and ~7.2×10^{-5} mol/s, respectively. HCl gas was vaporized at room temperature from a hydrogen chloride solution (2.0 M) in diethyl ether of which dose was ~2.6×10^{-4} mol/s. For purging the reactor, high purity N_2 gas (99.999%) was used with a flow rate of 400 sccm. All delivery lines were maintained at 120 °C. The specimen temperature was calibrated with a thermocouple-implanted 6 in. wafer in the temperature range of 50-400 °C. The base pressure of the reactor was less than 10 mTorr and ALD was processed at a working pressure range of 200-600 mTorr.

All thicknesses of the grown films were measured by a spectroscopic ellipsometer (SE, MG-1000, NanoView). The incident angle of the polarized light in the SE was fixed at around 70°, and the incident light has a spectral range of 1.5 ~5.0 eV. In order to determine an initial value of the thickness for fitting the measured data, it was firstly fitted with TiO_2 reference values of the real and imaginary parts of the complex dielectric function supplied by NanoView.[28] Subsequently the measured data were fitted with the Tauc-Lorentz dispersion function for all films.[29] Refractive index of the films was determined at 1.96 eV from the fitted parameters of the dispersion function.

By using five thicknesses obtained at center, top, bottom, left and right positions of the 6 in. substrate holder, non-uniformity of the grown film was evaluated by dividing the standard deviation of the thicknesses by the mean value.

X-ray diffraction (XRD) measurements were carried out in θ/2θ scan mode using a Philips X'pert Pro MRD X-ray diffractometer with Cu Kα emission.

In order to examine the electrical insulating properties of TiO_2 films, a capacitor structure of Au/TiO_2/native SiO_2 (2 nm)/*p*-Si(100) was fabricated by depositing 50 nm-thick Au films by thermal evaporation through a metal shadow mask for the top electrodes. The area of the Au electrode was ~1.26×10^{-3} cm^2. Leakage current -voltage characteristics of TiO_2 thin films was measured with a semiconductor parameter analyzer (HP 4145B).

Results and Discussion

Determination of Exposure and Purge Times. In order to determine the exposure time of $TiCl_4$ for the self-limiting growth, TiO_2 ALD was performed at 150 °C for 100 cycles with a sequence of $TiCl_4$ exposure – N_2 purging (30s) – H_2O exposure (1s) – N_2 purging (30s). The exposure time of water was fixed to be 1s of which the exposure time is generally enough for oxide films. As shown in Figure 1(a), the TiO_2 growth initially increases with the exposure time of $TiCl_4$, but saturates over 1s. By contrast, the poor non-uniformity at insufficient exposure times is dramatically improved by increasing the exposure time. Therefore the exposure time of $TiCl_4$ was determined to be 1s for the self-limiting growth.

The purging time for excess $TiCl_4$ and byproduct (*e.g.*, HCl) was also investigated in Figure 1(b) in which the ALD sequence of $TiCl_4$ exposure (1s) – N_2 purging – H_2O exposure (1s) – N_2 purging (30s) was repeated for 100 cycles at 150 °C. There is no severe variation in the TiO_2 thickness and non-uniformity even with shorter purging times than 1s. However we chose 5s as the purging time for the first-half reaction. Similarly, ALD experiments to determine the purging time for H_2O were performed at 150 °C for 100 cycles with a sequence of $TiCl_4$ exposure (1s) – N_2 purging (30s) – H_2O exposure (1s) – N_2 purging. Figure 1(c) shows that it takes much longer time in the second-half reaction than in the first-half reaction. We chose 20s to purge the excess water vapor and byproduct (*e.g.*, HCl). As a result, the optimized ALD sequence for TiO_2 was $TiCl_4$ exposure (1s) – N_2 purging (5s) – H_2O exposure (1s) – N_2 purging (20s).

Anomalous Effect of Growth Temperature on Growth-per-cycle and Crystallinity of TiO_2 Thin Films. Growth-per-cycle (GPC) of TiO_2 ALD was investigated in a temperature range of 100-400 °C as shown in Figure 2. The values of GPC were determined from the slopes in the plots of thickness versus number of cycles (100-400 cycles) at each growth temperature (data not shown). While typical ALD processes show a plateau of the GPC in an ALD temperature window, the GPC of our TiO_2 ALD from $TiCl_4$ and H_2O shows a large fluctuation in which a maximum (0.75 Å/cycle) and a minimum (0.42 Å/cycle) appear at 200 and 300

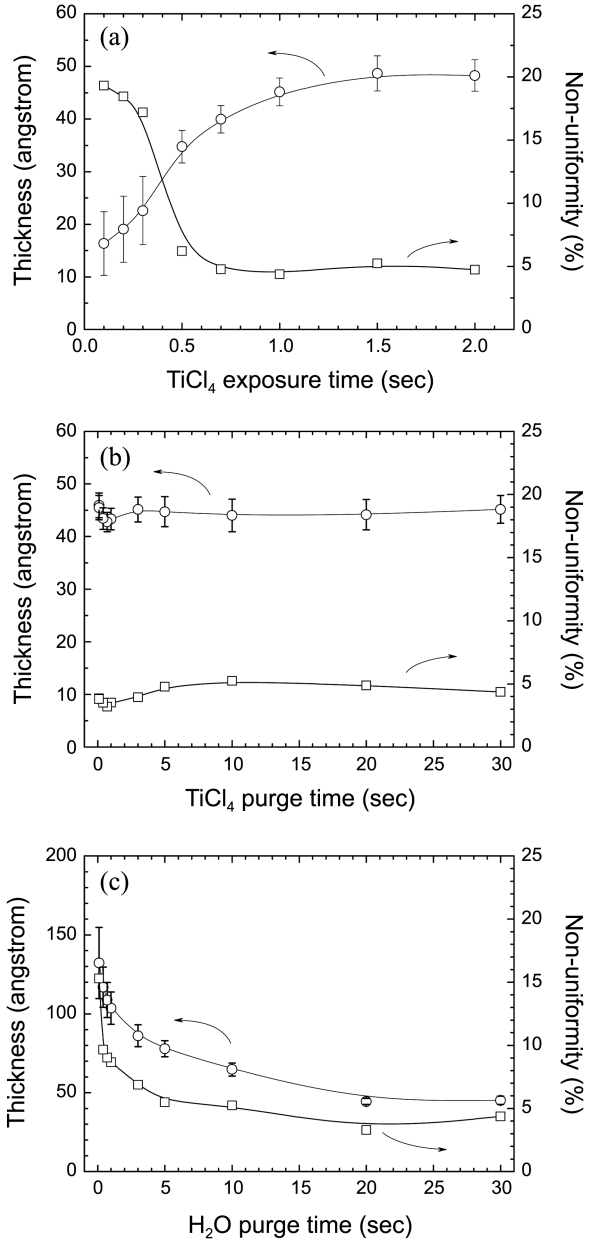

Figure 1. Thickness (circles) and non-uniformity (squares) variations as a function of $TiCl_4$ exposure time (a), $TiCl_4$ purge time (b), and H_2O purge time (c) in TiO_2 ALD at 150 °C for 100 cycles. The error bars in the circles denote the standard deviations of TiO_2 thicknesses grown at top, bottom, left, right and center positions in a 6 in. wafer.

°C, respectively. The GPC increases by a factor of 1.8 when the growth temperature is raised from 200 to 300 °C. Aarik, *et al.* also observed the anomalous increase in the GPC in a temperature range of 175-225 °C in ALD of thick TiO_2 films for which the number of cycles was 3000 cycles.[23] They proposed that crystallization of TiO_2 results in surface roughening and increase in surface area. Larger amounts of precursors are adsorbed on the surface, and consequently an additional increase in the GPC is obtained. However they reported that no similar behavior was observed in thinner films than 20 nm because the crystal structure was not

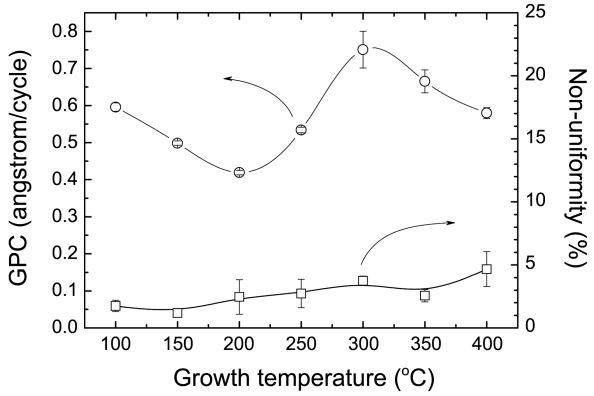

Figure 2. GPC (circles) and non-uniformity (squares) variations as a function of growth temperature. The error bars in the circles denote the standard errors in the linear fitting of the grown thicknesses with respect to the number of cycles. The error bars in the squares denote the standard deviations of the non-uniformity.

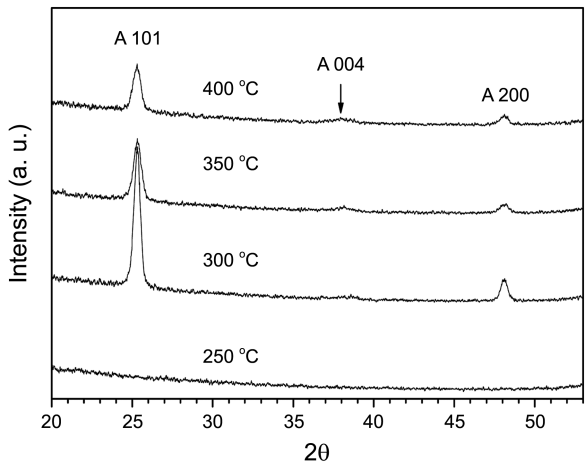

Figure 3. XRD patterns of TiO_2 films grown at 250-400 °C, of which thicknesses are ranged in 20-24 nm. The peaks were identified as those of the anatase (A) phase.

developed yet for small number of cycles at the low growth temperatures.

Figure 3 shows XRD diffraction patterns for TiO_2 films of which thicknesses are ranged from 20 to 24 nm. The film grown at 250 °C was amorphous due to the thin thickness while, in the Aarik's reports,[23,25] the crystalline anatase peaks was observed even at 150 °C from thick TiO_2 (3000 cycles). The GPC value (0.53 Å/cycle) at 250 °C is significantly larger than that (0.42 Å/cycle) at 200 °C even though both films are amorphous. Thus the anomalous increase in GPC at 200-300 °C cannot be explained only by the increase of the surface area due to the crystallization. The other factors for the anomalous tendency of the GPC will be explained in the following section.

One more concern in the XRD pattern is that the intensity of the anatase peak (101) is unusually attenuated at higher growth temperatures. Figure 4 shows refractive index of TiO_2 films deposited at each growth temperature. Considering the refractive index of thin films is directly related to

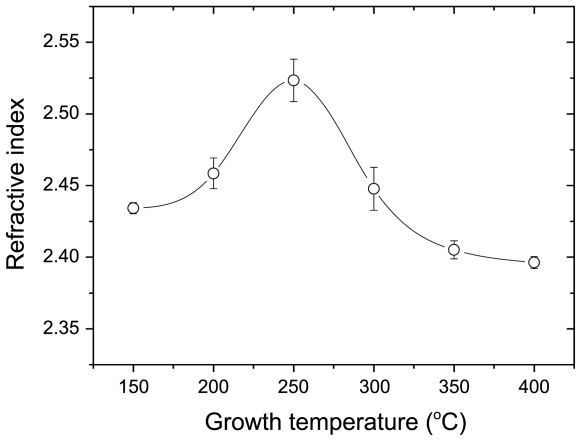

Figure 4. Refractive index variation as a function of growth temperature. The error bars denote the standard deviations of the refractive indices obtained at top, bottom, left, right, and center positions in a 6 in. wafer.

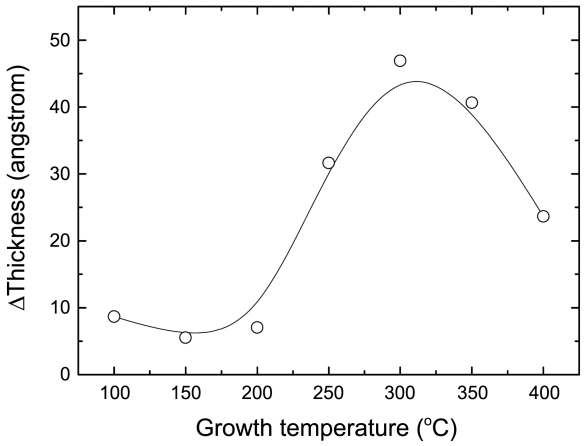

Figure 6. Δ thickness as a function of growth temperature: the Δ thickness is defined as a thickness difference by subtracting the thickness grown for 100 cycles (*i.e.*, circles in Fig. 7) from the thickness calculated by the GPC in Figure 2.

density of them, it should be noted that the density increases from 150 to 250 °C, but unusually decreases from 250 to 400 °C. Because the films grown at 150-250 °C are amorphous, they may become denser at higher temperatures. However the decrease in the density at 250-400 °C is abnormal, which may be related to the degree of crystallization in the TiO_2 films. Electrical insulating properties of TiO_2 films shown in Figure 5 also support the results of XRD and refractive index. The amorphous film grown at 150 °C shows the lowest leakage current density due to the absence of a leakage path through grain boundaries. The grown film at 300 °C shows poorer insulating characteristics than the film at 400 °C, because the film at 300 °C is more crystallized than that at 400 °C as shown in Figure 3.

Generally the GPC of ALD is not constant with respect to the ALD cycles, but it can be varied with the number of cycles. In an initial stage of ALD cycles, the underlying substrate (*e.g.*, SiO_2/Si) is generally dissimilar to the growing layer (*e.g.*, TiO_2). Therefore the GPC is also different between the early and late stages of ALD cycles. In addition, if the growing layer can be crystallized as deposited, the GPC of the early stage will be smaller than that of the late stage because TiO_2 grown at the early stage is amorphous. The GPC of the Figure 2 was obtained from the slope of a plot of the grown thickness versus the number of cycles in a range of 100-400 cycles. Therefore the GPC in Figure 2 may represent the growth behavior at the later stage than at the early stage.

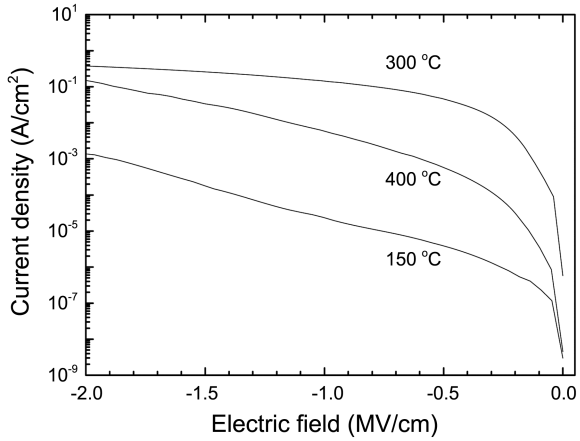

Figure 5. Electrical insulating properties of TiO_2 films grown at 150, 300 and 400 °C.

Figure 6 shows the difference (Δ thickness) between the calculated thicknesses with the GPC in Figure 2 and the experimental thicknesses (shown with open circles in Fig. 7) for 100 cycles. Below 200 °C, there is no significant difference between the calculated and experimental values. This reveals no significant change in the growth behavior between the early and late stages of ALD cycles. However the Δ thickness shows a clear parabolic variation at higher temperatures than 200 °C. The positive value of Δ thickness means that the thickness grown for 100 cycles at the early stage of ALD process are thinner than the thickness grown for 100 cycles at the later stage.

As Aarik, *et al.* explained the abnormal increase of the GPC with crystallization,[23] the variation of Δ thickness can be explained with progress of crystallization which results in an increase of the surface area (*i.e.*, adsorption sites). Below 200 °C, TiO_2 is amorphous. Thus Δ thickness is negligible, since TiO_2 is not crystalized in both early and later stages. The decreasing tendency of the GPC (below 200 °C in Fig. 2) in the amorphous TiO_2 growth is typical and similar to that in the Al_2O_3 ALD in which the phase is also amorphous. On the other hand, the anatase structure of TiO_2 is well developed at 300 °C and Δ thickness shows its highest value. Furthermore, as the anatase peak becomes smaller (above 300 °C in Fig. 3), Δ thickness also decreases. This strongly supports that the GPC is severely influenced by the crystallization. However, the anomalous increase of the GPC and Δ thickness at 200-300 °C cannot be explained by only crystallization, because TiO_2 grown at 250 °C is still amorphous according to the XRD pattern.

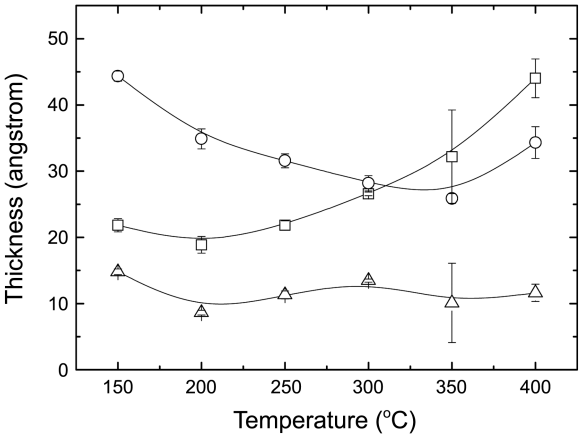

Figure 7. Thicknesses of TiO_2 films as a function of growth temperature. The films were grown for 100 cycles by three kinds of ALD processes. Circles (Typical ALD): $TiCl_4$ exposure (1s) – N_2 purge (5s) – H_2O exposure (1s) – N_2 purge (20s); squares (Modified ALD, M'): $TiCl_4$ exposure (1s) – N_2 purge (5s) – HCl exposure (1s) – N_2 purge (5s) – H_2O exposure (1s) – N_2 purging (20s); triangles (Modified ALD, M''): $TiCl_4$ exposure (1s) – N_2 purge (5s) – H_2O exposure (1s) – N_2 purge (20s) – HCl exposure (1s) – N_2 purge (5s).

Role of HCl in TiO_2 ALD. Recently, Matero *et al.* investigated the mechanism of TiO_2 ALD from $TiCl_4$ and water by using *in-situ* quadrupole mass spectrometry (QMS) and quartz crystal microbalance (QCM).[8] The ALD growth mainly proceeds *via* exchange reactions (Eqs. 1-2) on the surface. When the growth temperature is increased from 150 to 250 °C, the number (n) of –Cl ligands, released during the $TiCl_4$ pulse, decreases from about two to one (from bifunctional to monofunctional adsorption). However, at temperatures higher than 250 °C, less than one –Cl ligand (n < 1) is released, indicating that the dissociative chemisorption of $TiCl_4$ on the oxygen bridges (Eq. 4) also contributes to the first-half reaction. The formation of oxygen bridges *via* the dehydroxylation (Eq. 3) of OH groups is generally more preferred at higher temperatures. Thus the dissociative chemisorption may more contribute to the first-half reaction of TiO_2 ALD at higher temperatures. Therefore we may infer a relation between the GPC and the dissociative chemisorption of $TiCl_4$.

In recent, Turner *et al.* reported density functional theory (DFT) calculations of the initial surface reactions of TiO_2 ALD on SiO_2 substrate.[12] According to the DFT calculations, the first half-reaction *via* monofunctional chemisorption between SiOH and $TiCl_4$ is slightly exothermic with an enthalpy change of around –0.28 eV, which is a much smaller value comparing to the first-half reaction of Al_2O_3 between AlOH and TMA (–1.70 eV).[4] Furthermore the bifunctional chemisorption is rather endothermic with an enthalpy change of ~0.017 eV. Therefore we should consider reverse reactions (*i.e.*, desorption) of chemisorption in order to understand the growth behavior of TiO_2. The reverse reaction may results in decrease of GPC. In general, each half-reaction of ALD is not in equilibrium due to short pulse times of precursors and purging steps by inert gas. If the gaseous byproduct is efficiently removed by the purging step, the chemisorption may be thermodynamically favored than desorption. However considering the non-equilibrium nature of ALD process, the reverse reactions (desorption of precursors) cannot be excluded in a practical point of view. Therefore the monofunctional and bifunctional adsorption (Eq. 1) in the first-half reaction is non-ideal chemisorption for ALD process, especially under the presence of HCl. Different from the monofunctional or bifunctional chemisorption *via* ligand exchange reaction (Eq. 1), the dissociative chemisorption (Eq. 4) is highly exothermic (–1.21 eV) with a high activation of desorption (E_d = 1.56 eV)[12] and it is consequently irreversible and ideal for ALD process.

As a result, there are two ways for $TiCl_4$ chemisorption in the first-half reaction of TiO_2 ALD: ideal (irreversible) and non-ideal (reversible) adsorption. As proven by the QMS and QCM experiments,[8] as the growth temperature increases, the contribution of dissociative chemisorption of $TiCl_4$ increases but those of monofunctional or bifunctional chemisorption decreases in the growth of TiO_2. Therefore the anomalous increase of GPC and Δ thickness in the range of 200-300 °C can be explained by large contribution of the dissociative chemisorption.

In order to support the desorption of $TiCl_x$ species under the presence of HCl, we intentionally inserted HCl pulse after the first-half reaction in the typical sequence of TiO_2 ALD. The sequence of this modified ALD process (M') is $TiCl_4$ exposure (1s) – N_2 purge (5s) – HCl exposure (1s) – N_2 purge (5s) – H_2O exposure (1s) – N_2 purging (20s). The process M' was repeated for 100 cycles. Circles and squares in Figure 7 show the thicknesses of TiO_2 films by the typical and modified process M', respectively. Below 300 °C, the TiO_2 thickness by the modified process M' is thinner than that by the typical process due to the desorption of $TiCl_x$ by HCl. However the thickness difference between them becomes smaller at higher temperatures and then it interestingly becomes reversed above 300 °C. Because the irreversible dissociative chemisorption of $TiCl_4$ becomes gradually more favorable at higher temperature than 200 °C, the thickness reduction by the HCl pulse should be attenuated as the growth temperature increases. The reversal of the thickness difference above 300 °C in Figure 7 can also be explained as following: under HCl atmosphere, the desorption of $TiCl_x$ recovers OH groups, and the oxygen bridges become more dominant on the surface by the dehydroxylation of OH groups (Eq. 3). As a result, the larger coverage of the oxygen bridges may cause thicker TiO_2 by the irreversible chemisorption.

Another modified ALD process (M'') was also performed by inserting the HCl pulse after the second-half reaction in the typical sequence of TiO_2 ALD. The sequence of the modified process M'' is $TiCl_4$ exposure (1s) – N_2 purge (5s) – H_2O exposure (1s) – N_2 purge (20s) – HCl exposure (1s) – N_2 purge (5s). The process M'' was also repeated for 100 cycles. As shown in Figure 7 (triangles), the TiO_2 thicknesses by the modified process M'' are much thinner than those by the typical process or by the process M' in all temperatures.

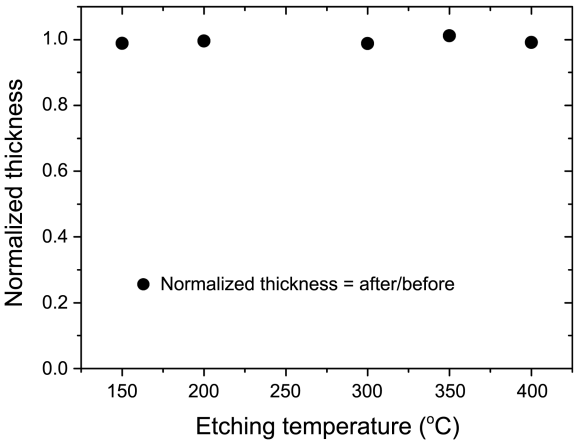

Figure 8. Normalized thickness of TiO_2 films as a function of etching temperature: the thickness after the etching was normalized by the initial thickness.

In an ideal case, all $TiCl_x$ species formed by the first-half reaction should be completely converted to $Ti(OH)_x$ or Ti-O-Ti in the second-half reaction. However if the reverse reaction (or re-adsorption of HCl) of the second-half reaction is possible, the $TiCl_x$ species may partially remain. Therefore TiO_2 growth will be retarded since the number of adsorption sites (-OH or oxygen bridges) for $TiCl_4$ is reduced in the subsequent first-half reaction. Indeed, according to the DFT calculations,[12] the second-half reactions (Eq. 2) are endothermic with a low activation of ~0.5 eV on the surface of both monofunctionally- and bifunctionally-chemisorbed $TiCl_x$. Therefore if the byproduct HCl is not efficiently removed or HCl is intentionally supplied after the second-half reaction (like the process M"), the TiO_2 growth is slower in comparison to the cases of the typical process or the process M'.

On the other hand, the dissociative chemisorption (Eq. 4) of $TiCl_4$ gradually more contributes to the growth of TiO_2 at higher temperatures, nevertheless the TiO_2 thickness is thin even at the high temperature region in the process M". This can be explained by the re-adsorption of HCl on the oxygen bridges as below:

$$\text{Ti(-O-)}_2\text{Ti(s)} + \text{HCl(g)} \rightarrow \text{Ti(Cl)-O-Ti(OH)(s)} \quad (5)$$

By the reaction of Eq. (5), the adsorption sites are converted from oxygen bridges to OH groups which may experience the similar chemistry mentioned in the previous paragraph. Therefore the growth of TiO_2 is severely retarded under the presence of HCl even at high temperatures.

Final concern for HCl is the possibility of etching of TiO_2 by the byproduct HCl during ALD process. In order to directly observe whether the etching by HCl is possible or not, we performed etching experiments (Fig. 8) in which 30 nm-thick TiO_2 film was exposed to HCl for 1 sec and then purged for 5 sec. This sequence was repeated for 50 cycles at various temperatures. There is no significant change in thickness before and after the etching experiment in all temperatures. Generally etching is not an one-step reaction but a complex reaction in which many elementary reaction steps are included to form volatile species (*e.g.* $TiCl_4$). Therefore for the successful etching of TiO_2 by HCl, various reactions included in a series of the complex reactions should be favorable thermodynamically and kinetically. Considering the reversible nature of some reactions of the first- and second-half reactions, the etching may be kinetically hindered. Therefore the byproduct HCl does not etch the grown TiO_2 but simply bring about the reduction of adsorption site on the surface for the subsequent ALD step.

Conclusions

Here we investigated the role of HCl in the ALD of TiO_2 from $TiCl_4$ and water. In the first-half reaction of TiO_2 ALD, the hydroxyl groups and oxygen bridges on the surface compete for the chemisorption of $TiCl_4$. At low temperatures below 200 °C, the hydroxyl groups mainly play a role of adsorption sites, but the contribution of the oxygen bridge gradually increases as the temperature becomes higher. While the monofunctional or bifunctional chemisorption of $TiCl_4$ on the hydroxyl groups is reversible under the presence of HCl, the dissociative chemisorption on the oxygen bridges is irreversible. Therefore the GPC of TiO_2 ALD is severely dependent on the growth temperature. In addition, the second-half reaction of TiO_2 ALD is also reversible by the re-adsorption of HCl under the presence of HCl. Therefore, the byproduct HCl should be efficiently and completely removed in the purge steps to avoid a non-ideal ALD.

Acknowledgments. This paper was supported by Konkuk University in 2011.

References

1. George, S. M. *Chem. Rev.* **2010**, *110*, 111.
2. Suntola, T.; Antson, J.; Pakkala, A.; Lindfors, S. *SID 80 Dig.* **1980**, *11*, 108.
3. Suntola, T.; Hyvarinen, J. *Ann. Rev. Mater. Sci.* **1985**, *15*, 177.
4. Widjaja, Y.; Musgrave, C. B. *Appl. Phys. Lett.* **2002**, *80*, 3304.
5. Haukka, S.; Lakomaa, E. L.; Root, A. *J. Phys. Chem.* **1993**, *97*, 5085.
6. Kytokivi, A.; Haukka, S. *J. Phys. Chem. B* **1997**, *101*, 10365.
7. Schrijnemakers, K.; Impens, N. R. E. N.; Vansant, *E. F. Langmuir* **1999**, *15*, 5807.
8. Matero, R.; Rahtu, A.; Ritala, M. *Chem. Mater.* **2001**, *13*, 4506.
9. Aarik, J.; Aidla, A.; Mandar, H.; Uustare, T. *Appl. Surf. Sci.* **2001**, *172*, 148.
10. Schrijnemakers, K.; Cool, P.; Vansant, E. F. *J. Phys. Chem. B* **2002**, *106*, 6248.
11. Gu, W.; Tripp, C. P. *Langmuir* **2005**, *21*, 211.
12. Hu, Z.; Turner, C. H. *J. Phys. Chem. B* **2006**, *110*, 8337.
13. Methaapanon, R.; Bent, S. F. *J. Phys. Chem. C* **2010**, *114*, 10498.
14. Lakomaa, E. L.; Haukka, S.; Suntola, T. *Appl. Surf. Sci.* **1992**, *60/61*, 742.
15. Haukka, S.; Lakomaa, E. L.; Jylha, O.; vilhunen, J.; Hornytzkyj, S. *Langmuir* **1993**, *9*, 3497.
16. Ritala, M.; Leskela, M. Nykanen, E.; Soininen, P.; Niinisto, L. *Thin Solid Films* **1993**, *225*, 288.

17. Ritala, M.; Leskela, M.; Jhansson, L. S.; Niinisto, L. *Thin Solid Films* **1993**, *228*, 32.
18. Ritala, M.; Leskela, M.; Niinisto, L.; Prohaska, T.; Griedbacher, G.; Grasserbauer, M. *Thin Solid Films* **1994**, *249*, 155.
19. Aarik, J. Aidla, A.; Uustare, T.; Sammelselg, V. *J. Cryst. Growth* **1995**, *148*, 268.
20. Aarik, J.; Aidla, A.; Sammelselg, V.; Siimon, H.; Uustare, T. *J. Cryst. Growth* **1996**, *169*, 496.
21. Siimon, H.; Aarik, J. *J. Phys. D: Appl. Phys.* **1997**, *30*, 1725.
22. Sammelselg, V.; Rosental, A.; Tarre, A.; Niinisto, L.; Heiskanen, K.; Ilmonen, K.; Johansson, L. S.; Uustare, T. *Appl. Surf. Sci.* **1998**, *134*, 78.
23. Aarik, J.; Aidla, A.; Mandar, H.; Sammelselg, V. *J. Cryst. Growth* **2000**, *220*, 531.
24. Cameron, M. A.; Gartland, I. P.; Smith, J. A.; Diaz, S. F.; George, S. M. *Langmuir* **2000**, *16*, 7435.
25. Aarik, J.; Aidla, A.; Mander, H.; Uustare, T.; Schuisky, M.; Harsta, A. *J. Cryst. Growth* **2002**, *242*, 189.
26. Ferguson, J. D., Yoder, A. R.; Weimer, A. W.; George, S. M. *Appl. Surf. Sci.* **2004**, *226*, 393.
27. Triani, G.; Campbell, J. A.; Evans, P. J.; Davis, J.; Latella, B. A.; Burford, R. P. *Thin Solid Films* **2010**, *518*, 3182.
28. Thomas, M. E.; Tropf, W. J. In *Handbook of Optical Constants of Solids*; Palik, E. D., Ed.; Academic Press: San Diego, CA, 1998; p 653.
29. Jellison, G. E., Jr.; Modine, F. A. *Appl. Phys. Lett.* **1996**, *69*, 371.